ORCA – Online Research @ Cardiff

System-level integration tools for laser-based powder bed fusion enabled process chains

Pavel Penchev[1*], Debajyoti Bhaduri[2**], Luke Carter[3], Aldi Mehmeti[1], Khamis Essa[1], Stefan Dimov[1], Nicholas J.E. Adkins[3], Nathalie Maillol[4], Julien Bajolet[4], Johannes Maurath[5], Uwe Jurdeczka[6]

[1] Department of Mechanical Engineering, School of Engineering, University of Birmingham, Edgbaston, Birmingham, B15 2TT, UK

[2] School of Engineering, Cardiff University, Queen's Buildings, The Parade, Cardiff, CF24 3AA, UK

[3] School of Metallurgy and Materials, University of Birmingham, Edgbaston, Birmingham, B15 2TT, UK

[4] Innovation Plasturgie Composites, 2 rue Pierre & Marie Curie – 01 100 Bellignat, France

[5] OBE Ohnmacht & Baumgärtner GmbH & Co. KG, Turnstraße 22, 75228 Ispringen, Germany

[6] ALSTOM Transport Deutschland GmbH, Linke-Hofmann-Busch-Straße 1, 38239 Salzgitter, Germany

* Corresponding author

Email: p.penchev@bham.ac.uk

** Previously at the University of Birmingham at the time of manuscript submission.

Abstract

A multi-setup additive manufacturing (AM) platform that integrates the powder bed fusion (PBF) technology with a range of complementary pre- and post-processing steps has the potential to be an appealing and flexible production solution for addressing the technical requirements of the existing and new products. Especially, such multi-step manufacturing solutions could overcome the limitations of standalone additive, subtractive, replication and surface engineering processes by reinforcing their complementary capabilities. However, the lack of specially developed system-level tools to address interoperability issues in integrating PBF with other technologies leads to high uncertainty and overall risk in producing parts that incorporate geometries with different manufacturing requirements, e.g. parts with areas that can be cost-effectively machined while others require AM solutions. To address such open issues, this paper presents the development of generic hardware and software integration tools that can improve the system level performance of AM enabled process chains. In particular, the research reports the design and implementation of modular workpiece holding system and quality control strategy that can warrant the production of parts encompassing structures with distinctly different manufacturing requirements. An experimental validation of the proposed tools was performed to assess their capabilities in producing parts with high accuracy and repeatability. The results demonstrate that their synergistic utilisation can lead to significant improvements in producing AM sections on top of pre-machined preforms in regards to their positional accuracy and repeatability. It was observed that the positional accuracy in the hybrid additive-subtractive parts was improved thirtyfold with the system level tools from 0.604 mm and 0.442 mm to 21 μm and 10 μm along X and Y axes, respectively.

Keywords: Additive manufacturing, process chains, laser-based powder bed fusion, hybrid manufactured products, modular workpiece holding system, quality control strategy

1. Introduction

In the fast-evolving technology markets, new and innovative products are being continuously developed with significantly improved performance in order to meet the rising global consumer requirements for their greater efficiency, customisation and better quality [1]. At the same time, such novel products should be fabricated with more sustainable manufacturing technologies that are capable of delivering higher productivity rates, reduced energy consumption and material usage, and thus lesser environmental impacts [2]. Therefore, various manufacturing processes such as milling, electrical discharge machining (EDM), laser machining (LM), additive manufacturing (AM) and metal injection moulding (MIM) have been employed in fabricating new metallic products with continuously greater complexity as they can provide reliable and concurrently scalable solutions at relatively low manufacturing costs [3]. However, individual and/or stand-alone manufacturing processes often fail to deliver products that meet all the requirements concerning accuracy, geometrical complexity, surface integrity and manufacturing costs [3, 4]. This is due to their intrinsic technological limitations such as their capacity of processing certain materials only, inability to produce complex geometries or inhibitive production costs for use in high volume production [5]. Examples of such critical technological constraints of manufacturing processes include:

- The shapes and sizes of milling cutters introduce constraints with respect to the size and the geometrical complexity of features that can be fabricated, e.g. internal vertical edges have corner radius and thus the edge sharpness is greatly determined by the tool diameter. The reduction of tool diameter can adversely affect the removal rates and process robustness and hence can significantly increase the manufacturing costs due to tool wear and breakage. In addition, the smaller tools require machine tools that support higher spindle speeds, thereby maintaining the high-speed machining (HSM) conditions required by the latest generation of milling cutters [6]. Another important requirement that could be considered as a constraint too when HSM complex structures is the use of computer aided manufacturing (CAM) software. Especially, the efficient use of such CAM tools require experienced operators to select specialised HSM machining strategies and then to validate the generated HSM toolpaths [7].
- AM processes can produce complex geometrical features but in general manufacturing companies are reluctant to adopt this relatively new technology due to the following reasons: (i) its efficient use necessitates experience and skill sets that are substantially different from those required to operate conventional machine tools; (ii) the availability of data preparation tools for achieving a fully digital information flow between design, AM processes and other post-processing steps; (iii) in the majority of cases, near net shape parts require post processing operations to meet their surface integrity and accuracy requirements [8, 9]; (iv) the existence of metallurgical defects, such as residual stresses and internal porosity due to unmelted/partially melted powders and gas entrapment, which can significantly impair the material's mechanical properties [10]; (v) it is considered as a standalone process that is difficult to integrate with other necessary pre- and post-processing steps in existing manufacturing systems. As a result the AM processes are considered not sufficiently mature production solutions yet that can address the requirements of niche markets only, particularly for prototyping and small batch manufacture [11].
- MIM can be used to manufacture cost-effectively complex, near net shape metal parts in medium to large series which is typically more than 10,000 parts per year. A good dimensional control can be achieved while the surface finish, usually less than 1 μm (R_a), is sufficient in many application areas without any subsequent operations. Nevertheless, the MIM process has some limitations/constraints, such as: (i) high tooling costs and therefore a viable manufacturing alternative for producing medium to large series of parts only; (ii) any process flexibility for producing parts with small variations require more complex tooling concepts with exchangeable inserts; (iii) the MIM parts should have a planar bearing surface for placing them in sintering furnaces; (iv) in most cases MIM is not suitable for producing big parts due to difficulties in maintaining an acceptable dimensional accuracy, high material costs and the necessity to use bigger

sintering furnaces; (v) big variations in wall thicknesses can lead to deformations due to inhomogeneous shrinkage during sintering. Therefore, the MIM's efficient deployment require these constraints to be taken into account in part's design and thus to minimise the manufacturing cost without impacting on part's quality [12,13].

• Non-conventional technologies such as EDM and LM have relatively low material removal rates in comparison to mechanical machining processes and they often deliver a stochastic manufacturing performance due to the large number of process variables [14, 15].

The above mentioned limitations affect the capabilities of individual processes and thus the manufacturing options to meet the constantly growing requirements of the existing and newly immerging products. Therefore, the research community and industry have proposed more novel and flexible production solutions that integrate two or more technologies synergistically, referred to as hybrid manufacturing systems, to address their limitations as stand-alone processes [3-5, 16]. This is achieved by combining the capabilities of individual technologies and thus to capitalise on their complementarity. The literature review of hybrid manufacturing solutions reveals that the concept and its pilot applications have attracted considerable interest both from researchers and companies over the past ~10 years. Therefore, it is no surprising that a plethora of research efforts are focused now on developing this concept further and more importantly on its implementations in different contexts both by industry and academia [3-5, 16-18].

Combinations of laser-based additive manufacturing with subtractive machining processes (for example, micro-milling) are currently one of the important research and development directions in hybrid manufacturing. This is primarily due to these processes' capabilities of adding and removing material selectively with controlled resolution and thereby addressing geometrical complexity in parts (internal and overhanging features), while reducing the material wastage and excessive cutting tool usage simultaneously [16, 19]. The industrial uptake of such manufacturing solutions is also demonstrated through the introduction of a number of hybrid machine tools in the market, e.g. LASERTEC 3D hybrid from DMG Mori [20], INTEGREX i-400AM from Mazak [21] and Lumex Avance-25 by Matsuura [22]. Despite their high manufacturing flexibility, these machine tools also do have some important limitations arising from the integration of processes with fundamentally different physical characteristics in a single machine setup. For example, a hybrid system that combines powder bed fusion with precision milling in a single machine tool has to meet the operating conditions of both processes. While the additive manufacturing step would require a controlled environment in the machine chamber in order to avoid the parts' distortion and oxidation, the milling operation should accommodate the specific workholding sub-systems to withstand the cutting forces [23]. In addition, the productivity and cost-effectiveness of such combined manufacturing systems is greatly reduced because the integration of processes in a single set-up allows only one manufacturing technology to be active at a time [23]. The existence of metallurgical defects in the deposited material can also significantly impair the parts' mechanical properties [10].

In an attempt to resolve the limitations of single setup systems, researchers have turned their attention to multi-setup manufacturing solutions, also referred to as process chains or pilot production lines, where the capabilities of complementary manufacturing processes are combined through their sequential integration into multiple machine setups' production platforms. In this way, each manufacturing module can be optimised to address the specific performance requirements of an individual process rather than the requirements of all integrated manufacturing processes. So, the fundamental differences in the physical characteristics of integrated processes do not increase the engineering complexity of such multi-setup manufacturing solutions unnecessarily and therefore their overall cost does not increase considerably, compared to the single setup systems. Other important advantages of the process chain approach in combining manufacturing capabilities is that it can deliver much higher productivity due to the parallel utilisation of the integrated operations and provide the flexibility of synchronising the throughput of each manufacturing module [23]. However, despite these significant advantages over single setup hybrid AM systems, the industrial uptake of AM enabled process chains is yet to be realised.

The literature review also reveals that the research and development efforts focused on AM enabled process chains are scarce and even if AM pilot lines are proposed they do not offer the required level of reconfigurability to address the diverse manufacturing requirements of new and novel products with extremely complex geometrical designs [19, 23, 24-26]. This is mainly due to the lack of adequate system-level integration tools that can provide a seamless integration of all manufacturing modules in AM enabled production lines/platforms [19, 23, 24-27]. The importance of system-level integration tools for developing multi-setup manufacturing solutions has already been reported in the context of LM process chains [28]. In particular, it is demonstrated that the development of adequate hardware and software integration techniques can provide the required level of flexibility, accuracy and robustness to combine LM with a range of complimentary processes for the scale-up production of miniaturised parts such as complex signal filtering components for novel communication devices [29].

The aim of this research is the development of generic system level integration tools that can combine the proven standalone PBF technologies with a range of complementary pre- and post-processing steps in reconfigurable process chains. The next section introduces the proposed reconfigurable multi-setup AM enabled manufacturing platform and its critical requirements for system level integration tools. The development and implementation of generic system level tools are then presented which are subsequently validated for multi-setup AM production. Finally, the enabling capabilities of these system-level tools in deploying LPBF processes as modular technologies in multi-setup lines are discussed and conclusions are made.

2. System level integration tools for AM enabled process chains

2.1 Multi-setup AM manufacturing platforms

The processing steps of the proposed multi-setup AM enabled platform that combines laser-based powder bed fusion (LPBF) with subtractive machining processes, e.g. milling, is shown in Figure 1. LPBF was selected as a proven and widely used standalone AM process by industry for producing complex metal parts with its relatively better built resolution, dimensional accuracy, surface quality and design freedom in comparison to other AM processes such as directed energy deposition (DED) technologies [30-32]. As shown in Figure 1, the processing flow of the proposed multi-setup manufacturing platform could be summarised as follows: (i) the generation of a CAD model; (ii) process planning and CAM preparation, where the CAD model is split into sub-volumes. Some of them are for machining while the others are for AM, and thus to allow each of them to be produced cost-effectively owing to their specific shapes and technical requirements with respect to the integrated complementary technologies; (iii) the machining of the first volume that consists of solid sections from a block of material and thus to produce preforms for the follow up AM processing; (iv) scanning (data capture) of the machined preforms that can be considered optional as the preceding process can produce preforms with well-defined datum (reference position) for the successive AM step; (v) AM of the second volume on top of the machined preforms employing LPBF; (vi) second scanning of the hybrid part, which is also optional and depends on the requirements of the follow up processing step for "rest-volume" data, generated by comparing the workpiece with its CAD model; (vii) post-processing operations to meet technical requirements associated with geometrical accuracy, surface integrity and material's mechanical properties.
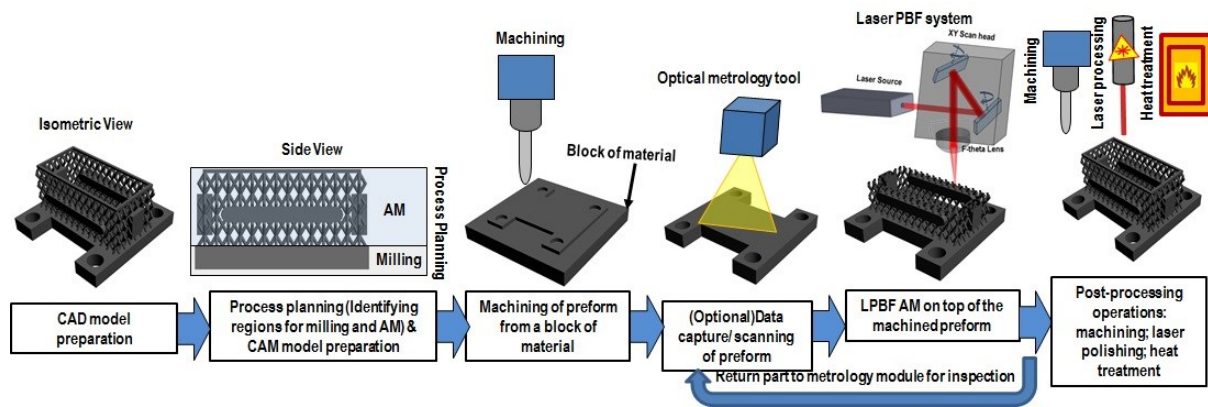
Figure 1. The processing steps of the laser-based process chain, which combines PBF with Machining

2.2 Critical requirements for system-level integration tools

It can be seen in Figure 1 that the successful utilisation of the AM enabled process chain necessitates the creation of both hardware and software integration tools that can ensure seamless interfacing of different processing steps. Despite the limited work reported so far on laser-based AM process chains, researchers have recognised the needs for such system-level integration tools with their direct impact on the manufacturing capabilities of multi-setup production platforms in regards to the cost-effective manufacture of complex parts with varying geometrical configurations and technical requirements [23, 27, 33]. The critical requirements for system-level hardware tools are primarily concerned with the accurate and precise repositioning of parts and thus to reduce or even eliminate time-consuming manual workpiece setting-up routines for different processing steps [23, 33]. At the same time, the critical requirements for the software tools are associated with the needs for: (i) ''smart'' process planning methods for splitting the parts' processing between subtractive and additive technologies integrated into the production lines and thus to autonomously identify the most time-efficient and cost-effective sequences of manufacturing operations [34-37]; (ii) product quality control strategies to ensure that parts' technical requirements are met at each processing step and thus to enable the early detection of parts' defects and also to prevent propagation of non-compliant products. It should be mentioned that the successful implementation of product quality control strategies requires the acquisition of product metrology data along the multiple processing setups. Such information should be used for a progressive correlation of workpieces' data to final part requirements/CAD data and hence to detect any deviations in regards to the orientation, dimensional and geometrical tolerances that can trigger defect-rectifying routines. The software integration tools reported in this paper are mainly focused on developing such product quality control strategies through the implementation of capabilities for an efficient product data analysis at the interfaces between the manufacturing steps of the proposed multi-setup platform. The next two sub-sections discuss the technical requirements of both hardware and software integration tools of these process chains.

2.2.1 Requirements for modular workpiece holding systems

The successful integration of LPBF processes into multi-setup manufacturing platforms is highly dependent on achieving a seamless interfacing of all processing steps with the required positioning and alignment accuracy and repeatability [23, 26]. While achieving such interfacing between the multiple steps, the deployed workpiece alignment methods can be both very time consuming and not sufficiently accurate due to the necessity to perform a registration of the workpiece's datum in each set-up by highly experienced operators [34, 38]. Furthermore, workpiece imperfections or defects can be a major cause for errors due to the use of different datum positions, fixtures, alignment devices and procedures in each processing setup of the production platform. Therefore, the following generic requirements were identified as critical and were taken into account when

designing a modular workpiece holding system for interfacing the multiple setups in the proposed production line with the needed accuracy, repeatability and reproducibility (ARR).

- High ARR achievable in positioning parts when interfacing the LPBF process with necessary pre- and post-processing steps;

- Modular workpiece holding device design based on standardised components for cost effective and robust implementation;

- Compactness and minimal height to minimise the loss of build height when integrating the workholding device in the LPBF build chambers;

- The necessity for common unifying interfacing solutions for integrating different modular technologies, e.g. for machining, LPBF, inspection and alignment, in process chains;

- The necessity to support both manual and automated workpiece setting up routines;

- Compatibility with different manufacturing processes and simple and fast integration in different multi-setup systems;

- Robust performance in harsh and abrasive environments, i.e. powder contamination in LPBF build chambers or the use of flood coolant during machining.

2.2.2 Requirements for software integration tools

The generic capabilities necessary for implementing advanced product quality control strategy should ensure that critical dimensional and geometrical tolerance requirements will be achieved in the proposed multi-setup production platform. These generic abilities should provide the pre-requisites for employing reliable product quality control strategies, in particular: (i) collection of traceable workpiece data with metrology modules at the interfaces between the manufacturing steps; (ii) processing tools for correlating data about workpieces to final part requirements/CAD data at the interfaces of the LPBF process with pre- and post-processing stages in the process chain; (iii) performing time-efficient feature-based geometrical reasoning and (iv) decision support tools for preventing the propagation of defects, process chain flow control, triggering defect rectifying routines and identifying shifts and trends in batches in regards to the parts' critical dimensions.

To create such generic capabilities the following specific requirements were identified as critical in designing system-level software tools for implementing the product quality control strategies in multi-setup platforms:

- The product quality control strategies and their associated system-level tools should employ broadly used and commercially available software solutions;

- Compatibility and connectivity to different metrology modules, i.e. 3D optical measurement devices or tactile measurement devices such as coordinate measuring machine (CMM);

- Support of different data formats, i.e. clouds of points, .stl files, and other neutral file formats;

- Necessity to support both manual and automated geometrical analysis of the collected metrology data;

- Different filtering techniques for selecting the most relevant and discriminant process parameters and critical part structures/dimensions/surface features for defect and out of control signal detection;

- Capabilities to perform robust and reliable alignment routines on the collected metrology data in pre-defined coordinate systems either on a global level, i.e. for the whole data set, or locally for selected data sub-sets only;

- Built-in capabilities for automatic and user-defined feature-based extraction and reasoning on various geometries (simple prismatic shapes, sphere, planes, cylinders etc.) employing the collected metrology data;

- Ability of correlating data about workpieces to final part requirements/CAD data and thus to extract 'rest' volumes [23-25] (remaining material stock for further processing) within a pre-defined tolerance levels.

3. Implementation of the system-level integration tools

3.1 Implementation of the modular workpiece holding system

3.1.1 Modular LPBF workholding device

Figure 2 depicts a schematic representation of a LPBF modular workholding device that was designed to address the requirements listed in section 2.1.1. It consists of commercially available standardised components that are well proven in different machining applications, whereas do not require frequent maintenance [30]. Figure 2(a) provides an exploded view of the LPBF workpholding device with all key components. In particular, it consists of main and secondary assembly units that are integrated into a protective chamber and thus to ensure robust performance in LPBF setups. The adequate sealing of the LPBF modular workholding device is achieved by fitting an O-ring on the top perimeter of the protective chamber that provides a tight fit between the main assembly unit and the bottom surface of the interface plate. In this way, the precisely machined mounting surfaces of the chuck, drawbar and pallet of the workholding device are satisfactorily protected from any undesirable contaminants such as chips/swarfs, cutting fluid during machining and powders during the LPBF processes. The incorporation into the design of a suitable protective chamber is especially important during the LPBF process, because the ball lock mechanism of the chuck can easily get stuck if there is not appropriate powder management solution in place [33] that can potentially lead to degradation of the workholding device's ARR. The main assembly unit as shown in Figure 2(c) incorporates the following components:

- a receiver (chuck) that can be precisely fixed and referenced either to a mechanical stage (rotary or linear) or the build substrate of a LPBF system and any other surface of the machine frame structure;
- a drawbar that provides means to precisely attach the pallet of the workholding device manually or automatically;
- A pallet that can carry the secondary assembly unit of the workpiece holding device.

The secondary assembly unit shown in Figure 2(b) incorporates workholding extensions, i.e. interface plates and adapters/extensions that can ensure the necessary flexibility in realising different processing setups while meeting the requirements for positioning and fixing workpieces with various geometrical designs and dimensions. As shown in Figure 2(b), examples of the integrated workholding extensions into the secondary assembly unit include:

- A plain interface plate;
- Interface plate with integrated vice for holding preforms with different geometrical designs produced with various manufacturing technologies, such as MIM and machining

- Chucks for holding axis-symmetric preforms that can be directly post-processed, e.g. by milling and/or by laser polishing/structuring/texturing, following the LPBF process, without removing the workpiece from the holding device for any follow-up processing with the required ARR.

The modularity of the proposed LPBF workholding device is ensured by using the same receivers (chucks) and pallets across all setups of the proposed production line. Thus, the workpieces have to be mounted only once onto the interface plate of the pallet and then carried throughout the entire sequence of the pre- and post-processing steps. In this way, the same workpiece coordinate system (WCS) can be preserved with regards to the receiver in each processing setup of the multi-stage platforms, as shown in Figure 3. It is worth mentioning that the positional repeatability of such workholding device is better than 1 μm [27], and thus it can provide highly precise workpiece positioning on multiple setups with the required ARR.
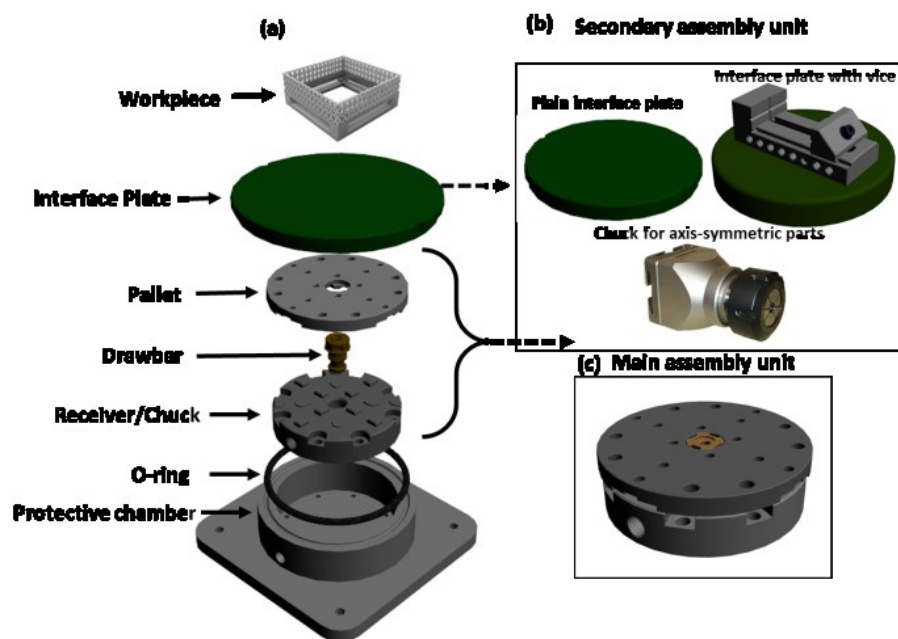

Figure 2. The schematic representation of the PBF modular workholding device for AM enabled process chains: (a) exploded view, (b) secondary assembly unit and (c) main assembly unit
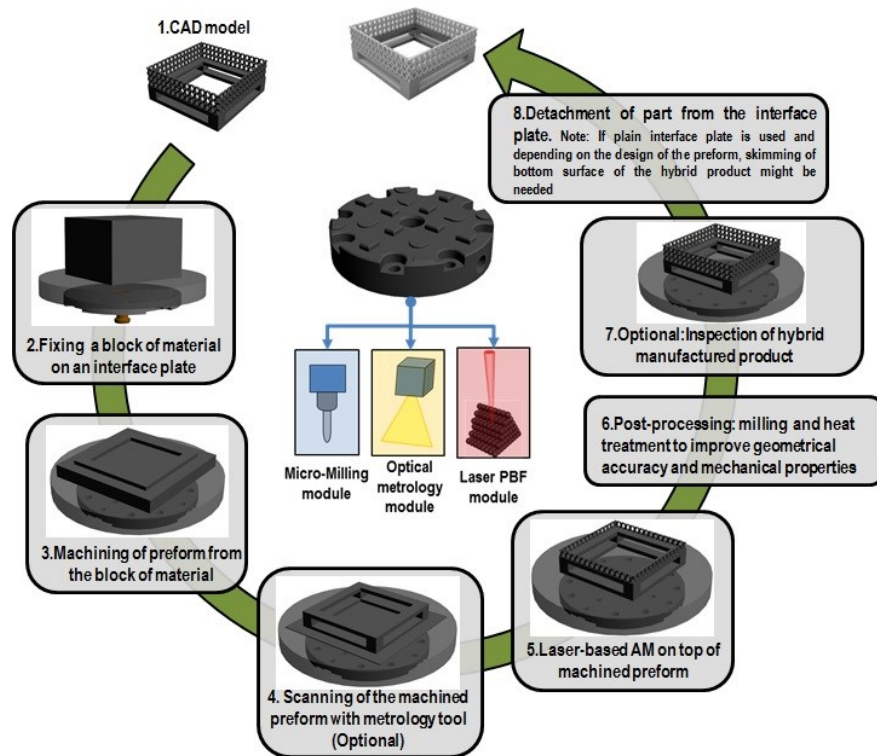
Figure 3. The use of a common workholding system across the multiple setups of the proposed LPBF enabled process chain

The next subsection 3.1.2 provides detailed information about the adopted approach for establishing a geometrical correlation between the coordinate systems of the modular workholding devices and processing modules in the proposed production line.

3.1.2   Setting up procedure

As outlined in Section 3.1.1, the modularity of the workholding system is ensured by having the same receiver (chucks) on all setups integrated in the manufacturing platform. This allows a common pallet to be used and transported between the different stages and thus to establish a geometrical correlation between the coordinates of the workholding system and that of each of the manufacturing modules in the platform. The setting-up of the chuck in the metrology and machining modules should be performed by using reference elements provided together with the components of the modular workholding devices following the procedures for correlating their coordinate systems to the modules' machine coordinate system (MCS), as defined by their manufacturers [39]. However, this referencing approach cannot be applied to laser-based PBF systems due to the lack of physical link between the processing tool, i.e. the laser beam, and any datum/components of the LPBF setup. In particular, an absolute geometrical correlation between the laser beam and the LPBF MCS cannot be established in the same way as on machining and metrology modules. This is because the sub-systems of such modules are physically linked to the frames of the machine tools through mechanical joints and their absolute positions, coordinates can be determined in MCS with the required ARR [27]. On the contrary, any laser beam pointing errors in the LPBF setup could lead to undesired shifting of the processed area in regards to the MCS and hence it will not be possible to achieve LPBF with the desired ARR. Factors that can negatively affect the geometrical correlation of the laser beam to MCS of the LPBF system include: (i) laser beam pointing instabilities caused by environmental factors such as large changes in temperature and humidity over a short period of time [28], (ii) changes in the optical beam delivery path such as the addition, removal or displacement of optical elements (i.e. mirrors) and (iii) deterioration of the calibration map of the employed focusing lens [40, 41].

Therefore, the establishment of a robust geometrical link between the chuck of the workholding system and the LPBF module require a specially defined referencing approach. Especially, a referencing procedure is necessary for finding the true position of the laser beam with respect to the workholding device coordinate System (WDCS) that will allow laser irradiation of preforms attached to a common pallet to be performed with required ARR.

A graphical representation of the step-by-step procedure for correlating WDCS to the coordinate system of the LPBF system (LMCS) is depicted in Figure 4. In particular, the reference procedure includes the following steps.
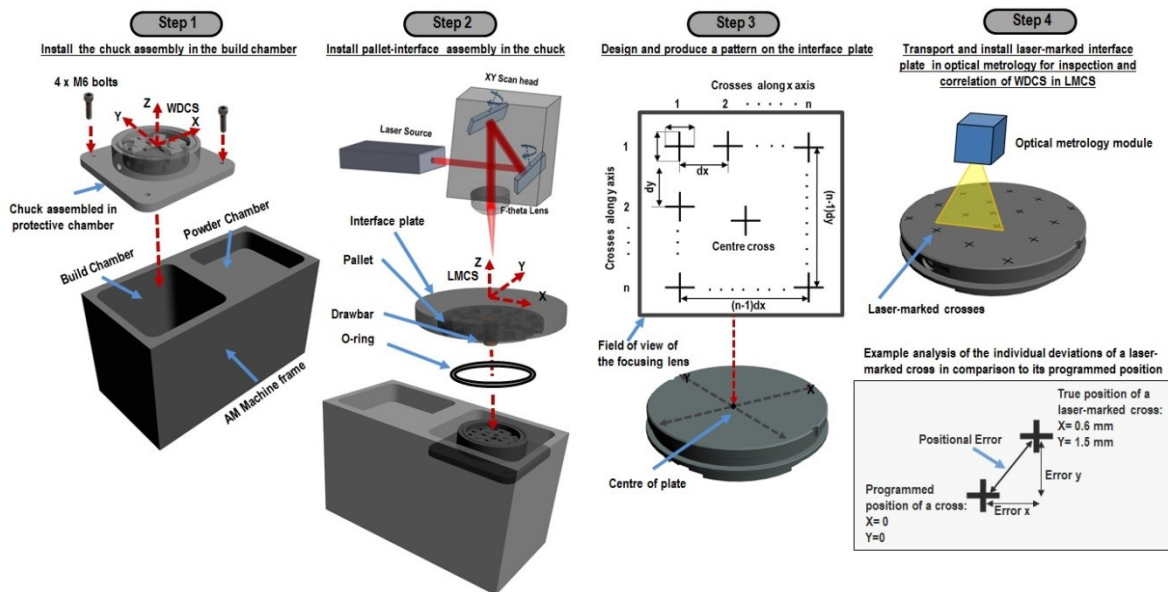

Figure 4. Graphical representation of the step-by-step procedure for referencing WDCS in LMCS

Step 1: The chuck is installed and secured by using screws into the protective chamber of the LPBF workholding device. When installing the chuck, it is important to follow a predefined sequence in tightening the fixation screws with the same torque and thus to ensure that the top surface of the chuck is parallel to the mounting surface of the protective chamber (a dial indicator can be used to check the parallelism when mounting the chuck). Then, the workholding device is installed and fixed into the build chamber of the LPBF machine using the fixation holes.

Step 2: A pallet representing a plain interface assembly is installed in the chuck via drawbar and is secured in place with a positioning accuracy and precision better than 0.002 mm [40]. LMCS determines the position of built parts in the LPBF module and the origin of LMCS is in the centre of the build chamber. However, it was already stressed that due to the lack of a physical link between the laser beam and any datum/components of the LPBF setup, the geometrical link between LMCS and WDCS is not known. Hence the latter has to be established in order to perform laser irradiation of preforms attached to a common pallet with the required ARR.

Step 3: A pattern consisting of simple geometries, i.e. crosses as reference marks that can fit within the field of view of the employed focusing lens, has to be designed. The target position of each reference mark is recorded by the control software of the LPBF system assuming that the LMCS coincides with WDCS, i.e. the centre of the interface plate's top surface. An example of a pattern with a series of crosses as reference marks which is designed and laser machined in the centre of a plain interface plate is shown in Figure 4 (step 3). In particular, the pattern consists of user-defined (n) number of crosses along the x and y axes of the interface plate with predefined nominal displacements *dx* and *dy*, respectively. In addition, there is one cross that is located at the centre of the pattern that represents the XY origin. Such a pattern could be used not only to correlate WDCS to

LMCS, but also to evaluate the positioning accuracy of the laser beam within the entire field of view of a given focusing lens. In this way, any local positional deviations of the laser beam, i.e. resulting from calibration errors, could be taken into account by applying the necessary positional compensation offsets when the processing/built files are generated. It should be also mentioned that the processing uncertainty could be reduced, especially the uncertainties associated with any local systematic positional errors across the focusing lens field of view, by reducing the distances between cross marks, i.e. dx and dy, while increasing their number.

Step 4: Releasing the pallet with the produced pattern from the LPBF module and installing it into the optical metrology module with a positioning accuracy and precision better than 0.002 mm to inspect the laser-machined crosses. Since WDCS is already referenced in the optical metrology module coordinate system (OMCS) the crosses' positional information is used to establish the geometrical correlation of WDCS in LMCS. In addition, the deviations of the laser-machined crosses from their programmed positions can be used to assess the positioning accuracy of the laser beam as explained in Step 3 and thus to apply positional compensation offsets when generating LPBF built/processing files. The application of such local beam positioning offsets is critical for obtaining the required level of ARR in the suggested production line.

3.2 Implementation of software integration tools

The dataflow approach adopted in the multi-setup manufacturing platform to enable the fabrication of complex parts that conform to their geometrical product specification (GPS) [42] is shown in Figure 5. The product quality control tools should allow the part's geometrical conformity after each processing step which should be monitored to ensure the implementation of the process chain flow control, i.e. for triggering defect rectifying routines and/or identifying shifts and trends in batches in relation to the parts' critical dimensions. It can be seen in Figure 5, that the input data for the product quality control tools include CAD and CAM models as GPSs as well as workpiece/part measurement data that are acquired throughout the processing steps of the AM enabled platform. In particular, the input data should allow to: (i) correlate the workpiece coordinate systems of parts to the coordinate system of processing modules and (ii) perform geometrical analysis by comparing data between the final part requirements/CAD data (according to GPS) and the measured/scanned parts (point clouds) after each processing stage. Such a comparison should allow workpiece/part features that do not conform to GPS to be identified as early as possible along the process chain in order to rectify defects or prevent their propagation.
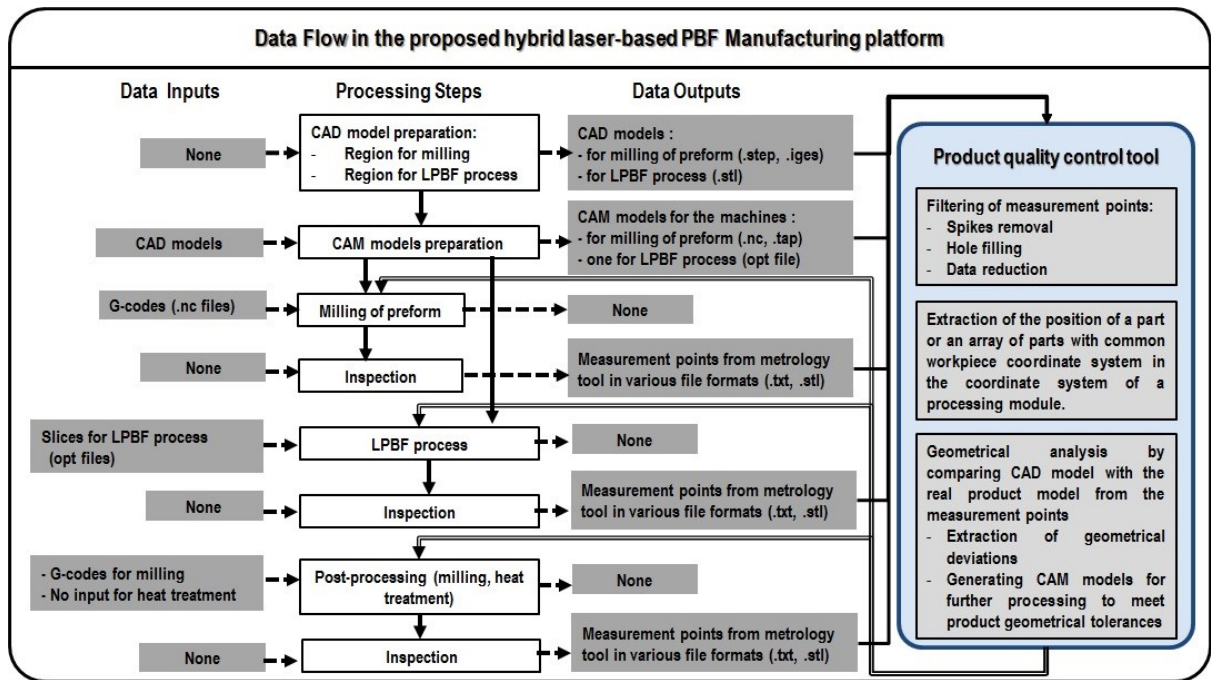
Figure 5. The dataflow approach of the proposed LPBF enabled manufacturing platform

The step-by-step procedure for implementing the product quality control tool when integrating LPBF processes with the necessary pre- and post-processing modules is depicted in Figure 6. It should be stated that due to the complexity and diversity of the steps constituting the product quality control tool, a number of commercially available software can be used to achieve its envisaged capabilities, e.g. GeoMagic Control X, AutoDesk PowerShape and PowerMill in this research. The description of how these software tools can be deployed is provided below for each step of the proposed quality control procedure.

Step 1. After the data capture employing an optical metrology module, the generated datasets are first filtered to minimise or even eliminate common problems, such as the existences of spikes, holes and noise, that can significantly impair the subsequent geometrical analysis. The filtering of measurement points should be performed directly on the metrology module employing suitable inspection software, e.g. GeoMagic Control X in this study that provides advanced algorithms for selecting the most relevant and discriminant metrology data.

Step 2. The filtered metrology data is imported into a CAD environment, e.g. AutoDesk Powershape, and then WCS is correlated to OMCS to obtain the workpiece position in LMCS. This is possible because a modular workholding system is used across all the processing modules of the multi-stage production line (see Section 3.1). Figure 6 exemplifies the extraction of the workpiece position in relation to OMCS. In particular, the horizontal displacement of the preform centre in regards to the OMCS is determined along the X and Y axes, respectively, together with the lateral preform rotation in the XY plane in regards to OMCS.

Step 3. The geometrical analysis of the scanned workpiece against its nominal CAD model and thus to extract volumes for further processing. In particular, the CAD model is imposed on top of the imported scan data as shown in Figure 6 and thus to identify volumetric geometrical deviations. As a result, "rest" volumes can be extracted for further processing and thus to meet the parts' GPS. Such geometrical analyses can be performed in suitable CAD environment, e.g. AutoDesk PowerShape in this research.

Step 4. The CNC programmes for the follow up processing module are generated based on the rest volumes obtained in Step 3. In particular, the extracted rest volumes should be imported into a CAM software, e.g. AutoDesk PowerMill in this research, and thus to generate the toolpaths for further processing.
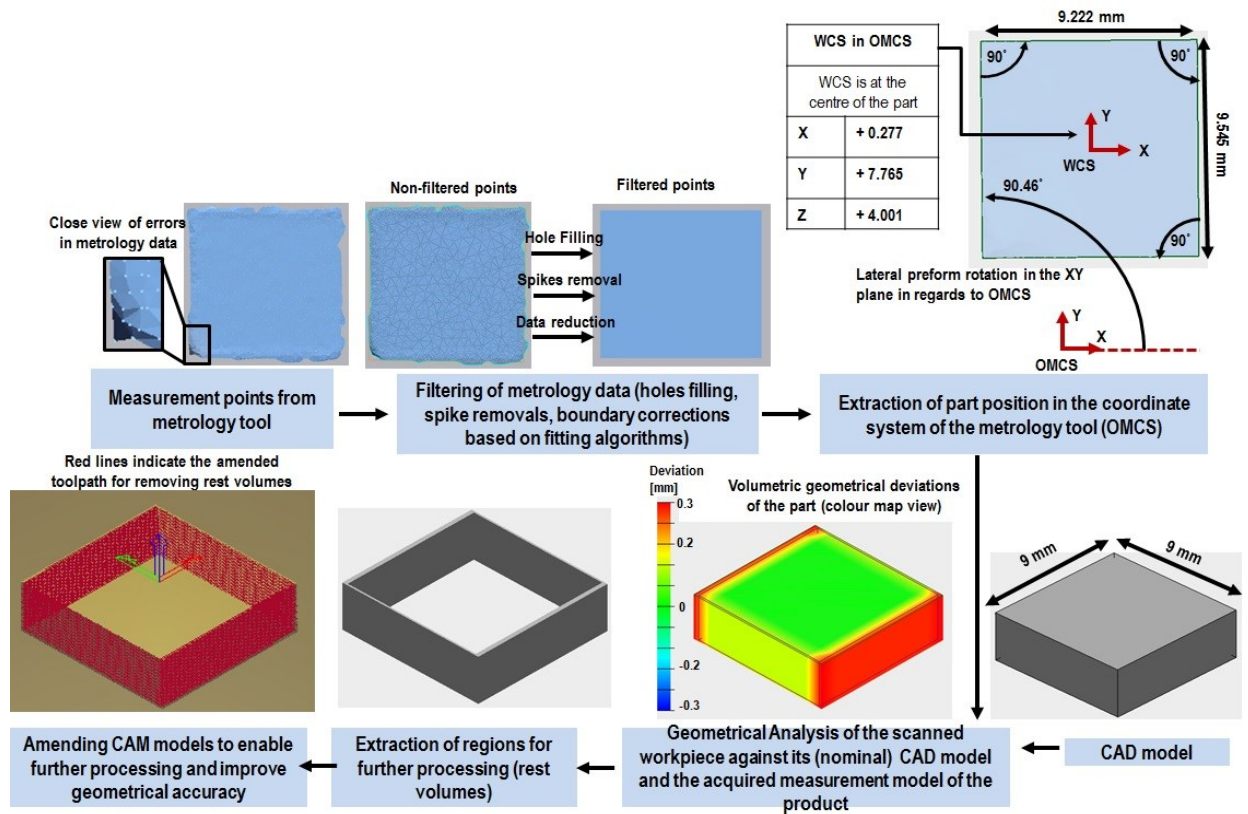
Figure 6. The step-by-step procedure for implementing the proposed product quality control strategy

4. Experimental validation

4.1 Methodology

The experimental validation of both the hardware and software system level tools was performed by producing the test part shown in Figure 7. The part was designed to fully cover the working envelop of the LPBF system used in the trials, which was a ConceptLaser M2 Cusing machine with a build volume of 250(X) x 250(Y) x 280(Z) mm that was filled with a protective gas environment to avoid any oxidation. Therefore, the test parts' overall dimensions were 245 (X) x 245 (Y) and 32 (Z) mm. In addition, The M2 LPBF machine was equipped with a 400 W fibre laser, a scanning head with a maximum beam deflection speed of 7 m/s and an F-Theta focusing lens to achieve a beam spot diameter of ~150 µm at the focal plane.

Aluminium A6082 alloy was used to manufacture the test part due to its excellent corrosion resistance and good machinability. Its front face incorporated 9 equally spaced protrusions that are 85 mm apart both along the X and Y axes with overall dimensions of 20 (X) x 20 (Y) x 15.5 (Z) mm and a 5 mm diameter through-hole in the centre (see Figure 7). The other side of the part had 15mm deep eight M8 and twelve M6 holes that were used to attach the test part to the pallet of the workholding device as shown in Figure 7. Five of the test protrusions were designed without any lateral rotation, while the remaining four protrusions were rotated around their centres at 15˚, 30˚, 45˚ and 60˚as depicted in Figure 7. In addition, the processing sequence of the test part protrusions was designed to validate the proposed multi-setup manufacturing approach. In particular, their 10 mm base sections were machined directly into the A6082 test part, while the 5.5 mm AM section on top of them was built using AlSi10Mg powder commonly used in LPBF systems. It is also worth mentioning that the dimensions of the AM sections were different (smaller), i.e. 17.5 mm (X) x 17.5 mm (Y) x 5.5 mm (Z) with a centre through-hole of 8

mm, compared to that of the machined base sections (preforms) on the test part. This was necessary in order to obtain a better access for inspecting the relative positions of the built AM sections with respect to the preforms. The AM sections were produced by using optimised processing parameters in another research [43], i.e. a laser power of 250 W, a scanning speed of 1500 mm/s, a scan space of 75 μm and an island size of 2 mm with a layer thickness of 30 μm [43]. The particle size of the AlSi10Mg powder was in the range from 20 to 63 μm with an average size of 35 μm. The obtained roughness (S_a) of their top surfaces was 5.5 μm, while that of the side walls was in the range between 8 and 10 μm.

To assess the capabilities of the system level tools to improve the manufacturing accuracy and repeatability of AM enabled multi-setup platforms, six of the test protrusions (2-4 and 6-8) were produced utilising the proposed tools, while the rest three (1,5 and 9) without the use of them. In this way, it was possible to assess clearly the impact of the system level tools on the achievable geometrical accuracy and repeatability in producing hybrid parts. It is important to mention that the three protrusions produced without the system level tools were selected to encompass the full size of the M2 PBF working field as shown in Figure 7 and thus to minimise the effects of the lens calibration error on the evaluation of the manufacturing accuracy and repeatability.

Figure 8 provides a graphical representation of the complete manufacturing sequence for producing the test part. The positional accuracy achievable with the proposed system level tools was assessed by measuring the positional deviations of the AM sections with respect to their machined preforms as shown in Figure 8. Ten measurements were performed on each of the nine hybrid protrusions. Furthermore, the positional repeatability was assessed by producing the test part twice. In particular, the AM sections were removed by machining following the first experimental trial in order to be produced again in the second test part. The repeatability of the suggested system level tools was determined by comparing the positional deviations of the AM cubes with respect to the machined preforms in the two trials. It should be noted here that the measurement of the nine machined preforms to obtain their respective positions in WDCS could be performed with a relatively low resolution metrology system, while the inspection of the hybrid parts should be carried out using a high resolution metrology system.
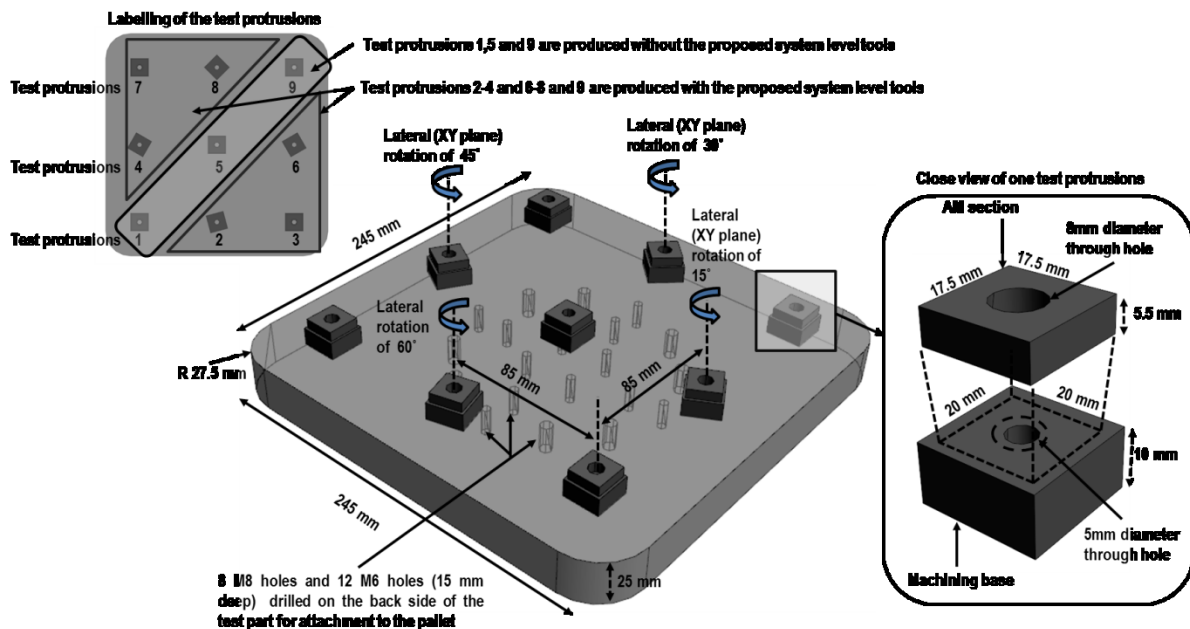

Figure 7. The test part for the experimental validation of system level tools
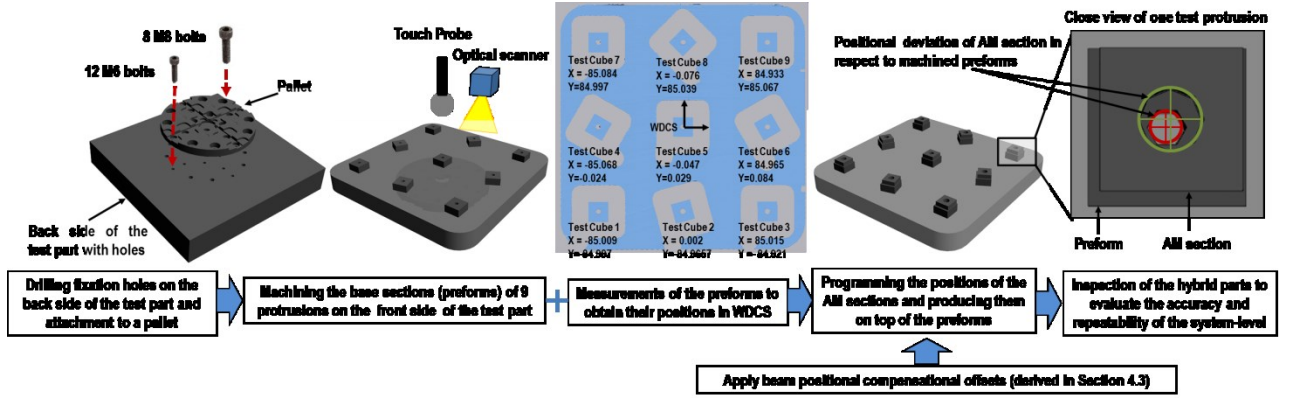
Figure 8. The processing sequence for the multi-stage manufacturing of the test part

4.2 Inspection systems

Two optical measurement systems were employed in the pilot implementation of the LPBF enabled process chain to obtain both high and low resolution metrology data. The acquisition of high resolution metrology data (a resolution higher than 25 µm) was performed with a Focus Variation (FV) optical microscope, namely Alicona InfiniteFocus (IF) G5. It has x5, x10, x20, x50 and x100 objective lenses that provide lateral resolution of 3.52, 1.76, 0.88, 0.64 and 0.44 µm, vertical resolution of 0.41, 0.1, 0.05, 0.02 and 0.01 µm and a repeatability of 0.12, 0.03, 0.01, 0.003 and 0.001 µm, respectively [44]. The system has an integrated precision stage with travel range of 100 mm in X, Y and Z, and thus to extend its measurement envelope beyond the lenses' fields of view. A maximum measurable height of 22 mm could be achieved with the x5 lens, while the maximum measurable area of the Alicona system is limited by the travel range of the integrated stages, which is 10000 mm^2 [44]. The acquisition of low resolution metrology data (lower than 25 µm) was performed with a 3D scan arm probe, namely Faro Edge ScanArm HD that was equipped with a hard touch-probe and a laser line probe. Its effective laser scan line length can be varied in the range from 80 to 150 mm by adjusting the distance between the measurement surface and the laser line probe, while there are 2000 measurements points per line [45]. The best measurement accuracy and repeatability achievable with the laser line probe is 25 µm when using the minimum scan width of 80 mm. The maximum measurement range of the Faro Edge ScanArm is 1.8 m [45].

The measurement uncertainty (U) was calculated according to Equations 1-3:

$$\bar{x} = \frac{\sum_{i=1}^{n} y_i}{n} \qquad \text{(Equation 1)}$$

$$sd = \sqrt{\frac{\sum_{i=1}^{n}(x_i - \bar{x})^2}{(n-1)}} \qquad \text{(Equation 2)}$$

$$U = \frac{sd}{\sqrt{n}} \qquad \text{(Equation 3)}$$

Where: sd is the standard deviation of the data set, x_i - the result of the ith measurement, n - the total number of measurements, and $\bar{x}$ - the arithmetic mean of the n results considered. It should be mentioned that the uncertainty calculations in this research were carried out based on ten repetitive measurements in accordance to the guidelines of the United Kingdom Accreditation Service (UKAS) [46].

4.3 Referencing and compensation procedures

The referencing of LMCS to WDCS is critical for achieving the desired level of positional accuracy in the proposed process chain as discussed in section 3.1.2. The test patterns were used to correlate LMCS with

WDCS of the M2 LPBF system and also to calculate its beam positional compensation offsets. The patterns included nine equally spaced 2mm long alignment crosses at 20 mm apart both in the horizontal and vertical directions. The centre cross (cross 5) coincides with the centre of the scanning field of the F-theta lens. Measurements of the test patterns were performed with the high resolution optical microscope (Alicona G5) with a x20 magnification lens that provided lateral and vertical resolutions of 0.88 μm and 0.05 μm, respectively. The measurement results for the nine laser marked alignment crosses for the M2 LPBF system are shown in Table 1. The positional deviations of the crosses in WDCS could be attributed to two error sources: one related to the positional correlation of LMCS in WDCS and one to the calibration errors of the F-theta lens. Therefore, the compensation offsets when programming the positions of the AM sections should include two components: one for the positional deviation of LMCS in relation to WDCS and the other for the F-Theta lens calibration errors.

The offset that corrects the lens calibration errors can be calculated by taking the absolute value of the average lens calibration error that can be determined by subtracting the nominal position of the crosses in LMCS from their measured position in LMCS. Figure 9 shows the plots of the focusing lens calibration errors both along X and Y axes for the working field of the M2 system used in this work. As expected, it increases with the increase of the offset from the centre of its F-Theta working field both along X and Y axes. For example, the average calibration error along Y axis is smaller than 15 μm when the y coordinate position is 0, while it is bigger than 50 μm both along the positive and negative directions when the offset from the centre is 20 mm. As it can be seen in Figure 9, a similar trend is observed for the calibration error along the X axis of the F-theta lens working field even though the average calibration error is relatively smaller. It is worth mentioning that, in order to assess the consistency of the calibration errors across the whole lens working field, an additional test pattern with 121 crosses was produced that covered an area of 200 mm (X) x 200 (Y) mm and the obtained results were in line with those from the smaller test pattern. Thus, the F-theta lens' working field is stretched about its centre with an average value of 0.039 mm and 0.048 mm along X and Y axes, respectively. Therefore, the compensation offset for the lens calibration errors along both axes is taken as the average of these two values, which is in particular 0.043 mm for the M2 LPBF system.

The compensation offset that correlates LMCS with WDCS can be calculated by taking the inverse of the average positional deviations of the crosses without the lens calibration errors. Figure 10 depicts the plots of the positional deviations for the M2 LPBF system used in this study that include both linear and rotational displacement components of the nine alignment crosses both along X and Y axes. The gradient of the linear fit to the plotted data represents the rotational displacement in radians, while the Y-intercept denotes the linear movement in mm. Based on the results in Figure 8, the positional correlation of LMCS with WDCS along the X and Y axes are defined by Equations 4 and 5, respectively.

$$WDCSx = -0.0026(LMCSx) - 0.522 \qquad \text{Equation 4}$$

$$WDCSy = 0.0026(LMCSy) - 0.324 \qquad \text{Equation 5}$$

In particular, the compensation offset to correlate LMCS with WDCS includes linear displacements of 0.522 mm and 0.324 mm along X and Y axes, respectively, and a rotational movement by 0.0026 radians (clockwise direction in XY plane) as stated in Table 1.

Table 1. Measurements results of the laser marked test pattern with the nine alignment crosses and calculation of compensation offsets for the M2 PBF system

| Parameter	Cross1	Cross2	Cross3	Cross4	Cross5	Cross6	Cross7	Cross8	Cross9
Nominal positions in LMCS									
X [mm]	-20	0	20	-20	0	20	-20	0	20
Y [mm]	-20	-20	-20	0	0	0	20	20	20
Average measured positions in WDCS (based on 10 measurements)									
X [mm]	-20.503	-0.469	19.602	-20.575	-0.527	19.546	-20.629	-0.592	19.463
Y [mm]	-20.440	-20.386	-20.332	-0.346	-0.319	-0.272	19.702	19.765	19.801
Average measured positions in LMCS (based on 10 measurements)									
X [mm]	-20.026	0.005	20.062	-20.053	0	20.058	-20.052	-0.018	20.037
Y [mm]	-20.047	-20.049	-20.050	0.031	0	0.001	20.067	20.078	20.058
Positional deviation (no lens calibration errors)									
X [mm]	-0.477	-0.474	-0.460	-0.522	-0.527	-0.512	-0.577	-0.574	-0.574
Y [mm]	-0.393	-0.337	-0.282	-0.378	-0.319	-0.273	-0.365	-0.313	-0.257
Lens calibration errors									
X [mm]	-0.026	0.005	0.062	-0.053	0	0.058	-0.052	-0.018	0.037
Y [mm]	-0.047	-0.049	-0.050	0.031	0	0.001	0.067	0.078	0.058
Compensation offsets in correlating LMCS to WDCS									
X [mm]					0.522				
Y [mm]					0.324				
Rotational angle about Z axis (in XY plane) [rad]					0.0026 (clockwise)				
Compensation offset to account for lens calibration errors in X and Y									
X&Y [mm]					0.043				
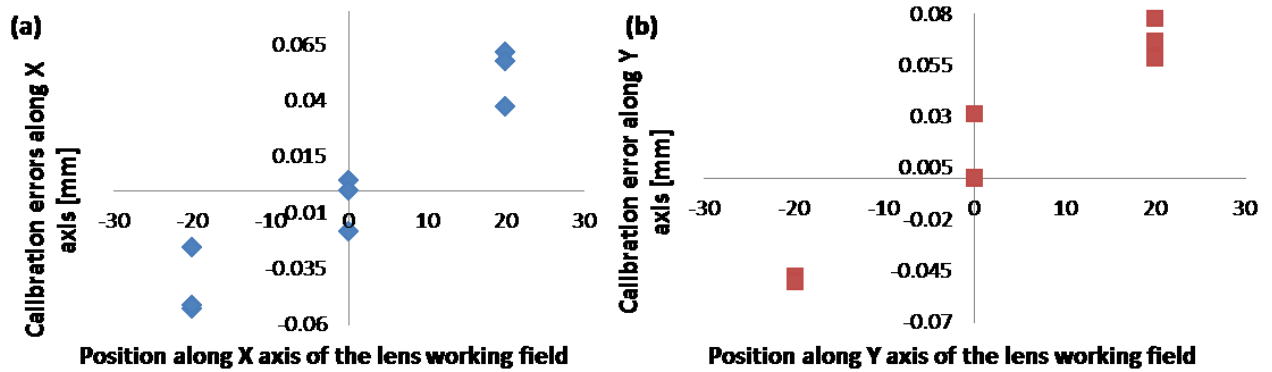
Figure 9. Plot of the focusing lens calibration errors (a) along X and (b) Y axes of the working field
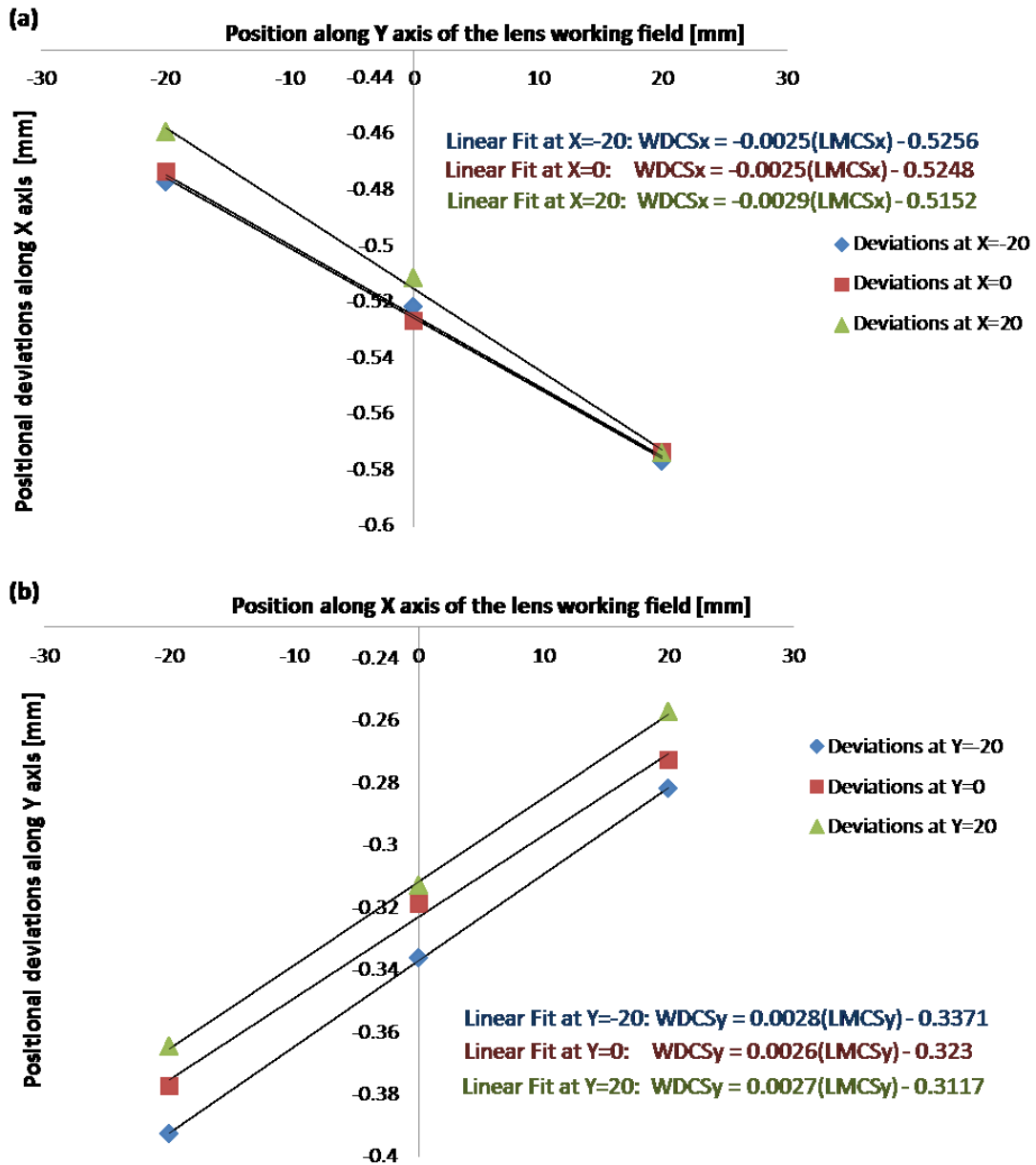
(a)

(b)

Figure 10. Plot of the positional deviations (without the lens calibration errors) of the nine alignment crosses along (a) X and (b) Y axes of the working envelope

5. Results and Discussions

Figure 11 depicts the processing steps of the multi-setup manufacturing sequence for producing the test parts described in Section 4.1. The modularity of the suggested workpiece holding device is demonstrated by installing receivers in each module integrated in the process chain and thus to carry the test parts throughout the entire AM enabled process chain without applying any process setting-up routines in its individual modules. Table 2 provides the measurement results obtained on the test parts after each step in the process chain. The positional accuracy of the preforms following their machining was within 90 µm with a measurement uncertainty of 2 µm, while the maximum deviations recorded for protrusions 6 and 8 were 88 and 80 µm along X and Y axes, respectively. Nevertheless, through the scanning step, the true positions of the preforms prior to the AM phase were obtained to mitigate the influence of machining errors on the positional / geometrical accuracy of the hybrid

parts. In addition, the application of beam positional offsets is critical for building the AM sections with the required accuracy and repeatability on top of the preforms as discussed in Section 4.1. Thus, Table 2 provides the final coordinates of the AM sections that should be taken into account when generating the files for the AM step. In particular, they include the positional compensation offsets calculated in Section 4.3 that account both for beam calibration errors and also for the misalignment of LMCS with respect to WDCS. In addition, Table 2 gives the measured positions of the nine AM sections in the two test parts that were subsequently compared to the preforms' positions to assess the achievable positional accuracy and repeatability with the system level tools in the multi-stage production line. The maximum measurement uncertainty for the AM sections was 5 µm, which was higher than that for the preforms even though they were inspected with the high resolution optical 3D microscope. This can be explained with the higher surface roughness of the AM sections in comparisons to the machined preforms.

Figure 12 shows the top views of the nine hybrid test protrusions from the first experimental trial. The positional errors of the AM sections in relation to the machined preforms are clearly visible. In particular, the three test protrusions (1, 5 and 9) that were produced without utilising the proposed system level tools exhibited much higher positional deviations in comparison to the others that were built using them. For example, it can be seen in Figure 12 that the AM sections of test protrusions 1, 5, and 9 are all shifted towards the bottom left corner in regards to the machined preforms. The observed positional deviations could be attributed to a number of factors including misalignment of WCS in relation to LMCS, beam calibration errors and inability to compensate the machining errors of the preforms originating from the pre-processing step. The lack of reliable and consistent referencing of WCS to LMCS is due to the high level of uncertainty in setting-up the laser-based PBF process, especially with the use of only four fixation holes to correlate the laser beam to the workpiece. Additionally, beam calibration errors are a common issue in any laser processing system that employs optical scanning heads and F-theta lenses to move the beam on the workpiece [41] and they could lead to significant deterioration of the machining accuracy. Nevertheless, the use of the proposed hardware and software system level tools to produce the other six test protrusions (2-4 and 6-8) resulted in substantial improvements in the positional accuracy of the AM sections with respect to the machined preforms as can be seen in Figure 12. In particular, the modular workpiece holding system provided accurate and precise positioning of the parts within the different modules of the multi-setup manufacturing platform. Besides, through the application of process and part related compensation offsets, the suggested quality control procedures can ensure the fabrication of parts conforming to their geometrical product specification requirements.

The positional deviations both along X and Y axes of the F-theta working field that were obtained for the nine hybrid test protrusions in the two experimental trials are provided in Figure 13. Especially, the deviation plots depict clearly the increase of the positional accuracy and repeatability achieved when the system level tools were deployed. For example, it can be seen in Figure 13(a) that the positional deviations along the X axis of the AM sections produced without the use of the system level tools were relatively systematic for all three protrusions and the maximum deviation of 0.604 mm was recorded in protrusion 9. Even though the deviations along Y axis are somehow smaller and less systematic than those observed for the X axis, it can be seen in Figure 13(b) that the maximum positional deviation recorded in protrusion 1 was as high as 0.443 mm. However, Figure 13 also reveals that the average positional deviations of the six AM sections produced with the system level tools in the two experimental trials were 21 µm and 10 µm along X and Y axes, respectively, while the maximum deviation of 43 µm was recorded in the X coordinate of protrusion 3 in the first experimental trial. The comparison of the results from the two experimental trials also unveils that the average positional repeatability with the system level tools along X and Y axes were 8 µm and 19 µm, respectively. It is worth mentioning that the positional repeatability of the three protrusions produced without the system level tools was comparable with that observed for the other six test protrusions as both test parts were mounted on the same modular workpiece holding device in the two experimental trials. Nonetheless, this is another evidence for the capabilities of the modular workholding system in ensuring reliable and repeatable repositioning of parts within the different modules of the manufacturing platform.

The results from the experimental study clearly show that the synergistic utilisation of both the software and hardware system level tools leads to considerable (more than thirtyfold) improvement in the positional accuracy and repeatability of the AM sections produced on top of the preforms in the two additive-subtractive test parts. It should also be noted that such positional accuracy is comparable with the processing resolution of the LPBF systems that typically produce parts with surface roughness in the range of 5 to 15 μm while their geometrical accuracy is usually within tens of microns [11, 43]. Therefore, the proposed system level tools can deliver high positional accuracy and repeatability when producing hybrid parts and thus can reduce the required geometrical tolerances for the post-processing operations and make them comparable with those for monolithic AM components. This implies considerable cost, energy and waste material savings when deploying the proposed AM enabled production line.

Table 2. Measurements results of the hybrid manufactured test parts produced in the two experimental trials
Notes: P1 to P9 denote the nine protrusions of the test parts

| Parameter	P1	P2	P3	P4	P5	P6	P7	P8	P9
Nominal position of test proportions' centres									
X [mm]	-85	0	85	-85	0	85	-85	0	85
Y [mm]	-85	-85	-85	0	0	0	85	85	85
The average positions of machined preforms' centres in WDCS (based on 10 measurements)									
X [mm]	-85.002	0.004	84.997	-85.046	-0.037	84.964	-85.068	-0.088	84.932
Y [mm]	-84.995	-84.971	-84.935	-0.022	0.029	0.080	84.997	85.033	85.058
U [mm]	0.002	0.001	0.002	0.002	0.001	0.002	0.002	0.002	0.001
Beam positional compensation offsets for the calibration errors of the F-theta lens									
X [mm]	0.043	0	-0.043	0.043	0	-0.043	0.043	-0	-0.043
Y [mm]	0.043	0.043	0.043	0	0	0	-0.043	-0.043	-0.043
Beam positional compensation offsets in referencing LMCS and WDCS (see Table 1)									
X [mm]	0.522								
Y [mm]	0.324								
Rotational angle [rad]	0.0026 (clockwise)								
Programmed positions of AM sections' centres in LMCS with all compensation offsets for both trials									
X [mm]	-85	0.305	85.254	-84.480	0	84.443	-84.279	0.650	85
Y [mm]	-85	-84.604	-84.791	0.523	0	0.18	85.499	85.314	85
Average measured positions of AM sections' centres in WDCS from Trial 1 (based on 10 measurement)									
X [mm]	-85.569	0.027	85.040	-85.052	-0.557	84.993	-85.051	-0.075	84.328
Y [mm]	-85.438	-84.976	-84.945	-0.033	-0.237	0.086	84.993	85.026	84.997
U [mm]	0.004	0.004	0.005	0.004	0.003	0.003	0.003	0.004	0.004
Average measured positions of AM sections' centre in WDCS from Trial 2 (based on 10 measurement)									
X [mm]	-85.546	0.036	85.032	-85.026	-0.548	84.989	-85.049	-0.089	84.323
Y [mm]	-85.401	-84.950	-84.919	-0.019	-0.226	0.088	85.012	85.055	84.999
U [mm]	0.003	0.003	0.004	0.005	0.004	0.004	0.003	0.003	0.004
Positional deviations of AM sections with respect to machined preforms in WDCS from Trial 1									
X [mm]	-0.567	0.023	0.043	0.006	-0.520	0.029	0.017	0.013	-0.604
Y [mm]	-0.443	-0.005	-0.01	-0.011	-0.266	0.006	-0.004	-0.007	-0.061
Positional deviations of AM sections with respect to machined preforms in WDCS from Trial 2									
X [mm]	-0.544	0.032	0.035	0.020	-0.511	0.025	0.019	-0.001	-0.609
Y [mm]	-0.406	0.021	0.016	0.003	-0.255	0.008	0.015	0.022	-0.059
Positional repeatability of the system level tools									
X [mm]	0.023	0.009	-0.008	0.014	0.009	-0.004	0.002	-0.014	-0.005
Y [mm]	0.037	0.026	0.026	0.014	0.011	0.002	0.019	0.029	0.002
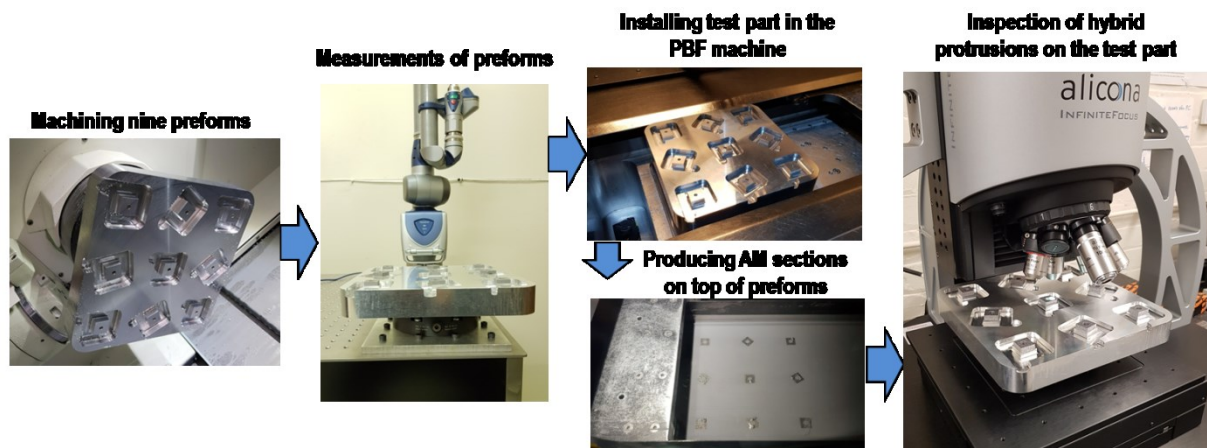
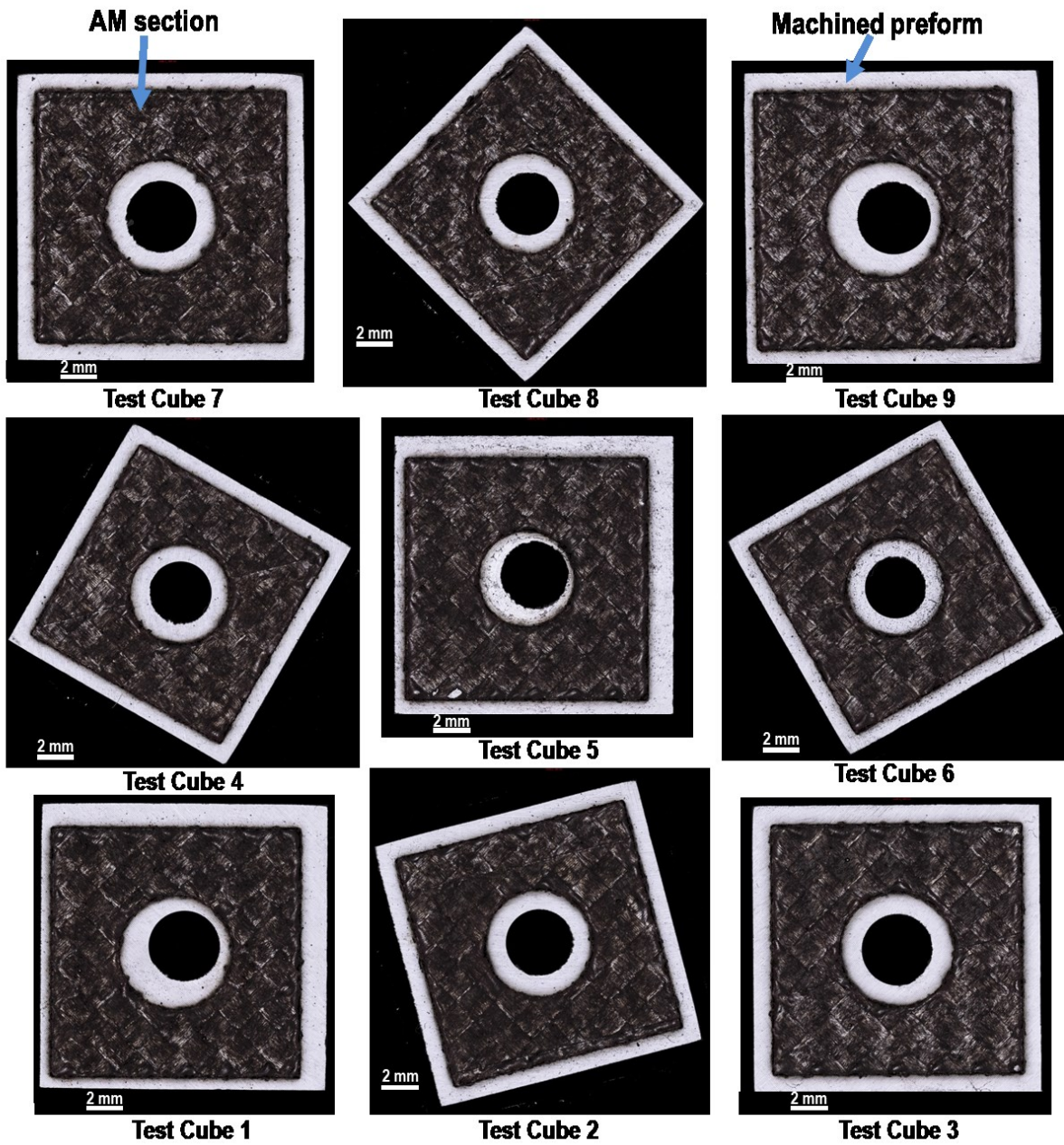Figure 11. Processing steps for the multi-stage manufacturing of the test part

Figure 12. Top views of the nine test protrusions to evaluate the positional errors of the AM sections with respect to their preforms
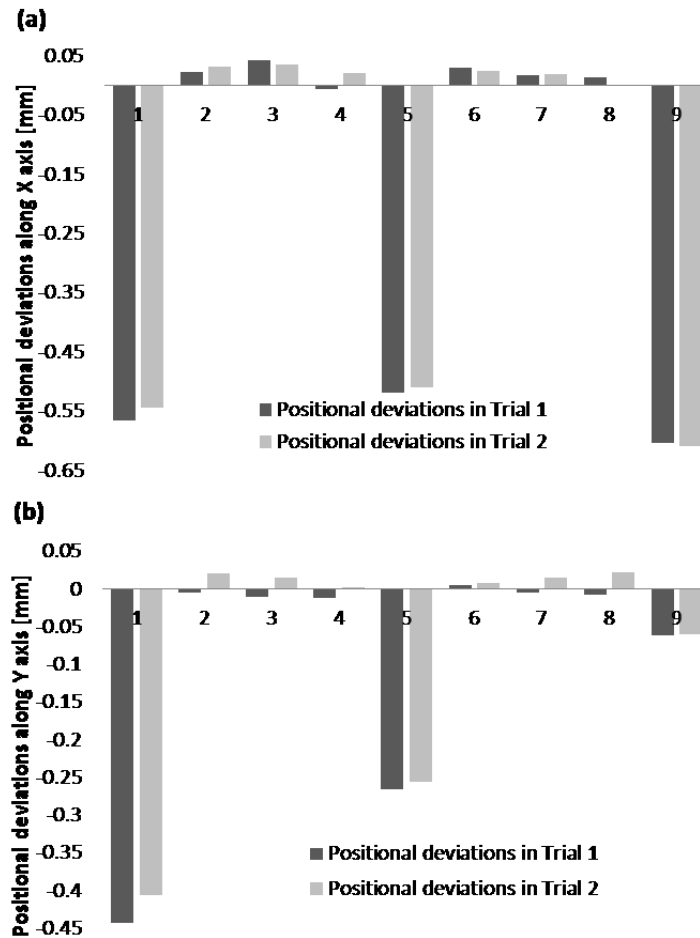
Figure 13. The plots of the positional deviations of nine AM sections with respect to the machined preforms in the two experimental trials along (a) X and (b) Y axes of the F-theta working field.

Note: In the plots, X axis denotes the test cube number, while Y axis provides the positional deviations in mm.

6. Conclusions

This paper presents the development of generic hardware and software system level tools for AM enabled multi-setup manufacturing platforms that can integrate proven standalone LPBF systems with a range of complementary pre- and post-processing technologies. In particular, the research reports the design and implementation of modular workpiece holding system and product quality control strategy that can enable the fabrication of hybrid parts that conform to their geometrical product specification requirements. The following conclusions can be made:

- The lack of sufficiently advanced system level integration tools in AM process chains leads to high positional deviations between the AM and machining sections of hybrid parts.
- The modular design of the proposed workpiece holding device for LPBF systems allows the precise and accurate repositioning of parts throughout the entire production line without the need to perform any setting up procedures for individual processing modules.
- The product quality control strategy when using system level tools underpins the fabrication of hybrid parts that conform to their product geometrical requirements. Especially, by deploying the suggested tools it is possible to minimise critical manufacturing errors in hybrid parts, i.e. positional misalignments

between their AM and machined sections. These errors are due to a number of factors such as misalignments in the working coordinate systems of the modules in the AM enabled multi-setup platforms, process specific errors, e.g. beam calibration errors in AM, and inability to monitor and rectify parts' geometrical unconformities after each processing step.

- The synergistic utilisation of both software and hardware system level tools can lead to significant improvements in the positional accuracy and repeatability when producing AM sections on top of the preforms in hybrid parts. In particular, it was observed that positional accuracy in the hybrid parts was improved thirtyfold with the system level tools, from 0.604 mm and 0.442 mm to 21 µm and 10 µm along X and Y axes, respectively.

- The capabilities of the proposed system level tools to deliver high positional accuracy and repeatability in hybrid parts implies considerable cost, energy and waste material savings when deploying the suggested AM enabled process chain.

Acknowledgements

References

1. Zwan R. Technologist versus "Technologee": The problem of communication between users and developers of complex products. In: Current trends in technology and society-Volume 1.Primrose Hall Publishing Group, 2012, pp.46-58.
2. European Commision. Horizon 2020 Work programme 2016-2017: Cross- Cutting Activities, July 2016 , https://ec.europa.eu/research/participants/data/ref/h2020/wp/2016_2017/main/h2020-wp1617- focus_en.pdf
3. Chu WS, Kim CS, Lee HT, Choi JO, Park JI and et al. Hybrid Manufacturing in Micro/Nano Scale: A Review. Int. J.Precis. Eng. Manuf.-Green Tech. 2014; 1(1): 75-92.
4. Lauwers B, Klocke F, Klink A, Tekkaya AE, Neugebauer R, McIntosh D.Hybrid Processes in manufacturing. Annals of the CIRP. 2014; 63(2):561–583.
5. Newman ST, Zhu Z, Dhokia V and Shokrani A. Process planning for additive and subtractive manufacturing technologies. CIRP Ann. – Manuf. Technol. 2015; 64 (1): 467-470.
6. Z. Wang M. Rahman. High-Speed Machining, Reference Module in Materials Science and Materials Engineering Comprehensive Materials Processing 2014; (11):221–253.
7. Patel Divyangkumar Dharmendraa, D.I.Lalwanib. A Spiral Toolpath for Machining of Elliptical Pockets Using Partial Differential Equation. Materials Today: Proceedings 2015; (2) 3394 – 3402   .
8. Quan Z and et.al. Additive manufacturing of multi-directional preforms for composites: opportunities and challenges. Materials Today 2015; 18: 503–512.
9. Shah P, Racasan R and Bills P. Comparison of different additive manufacturing methods using computed tomography. Case Studies in Nondestructive Testing and Evaluation 2016; 6:69-78.
10. Gorsse S, Hutchinson C, Gouné M & Banerjee R.Additive manufacturing of metals: a brief review of the characteristic microstructures and properties of steels, Ti-6Al-4V and high-entropy alloys. Science and Technology of Advanced Materials 2017; 18(1): 584–610.
11. Duck Bong Kim, Paul Witherell , Robert Lipman, Shaw C. Feng. Streamlining the additive manufacturing digital spectrum: A systems approach. Additive Manufacturing 2015; (5): 20–30.
12. Dehghan-Manshadi A, Bermingham MJ, Dargusch MS,StJohn DH and Qian M. Metal injection moulding of titanium and titanium alloys: Challenges and recent development. Powder Technology 2017; 319: 289-301.

13. Burkhardt C, Die Bibliothek der Technik 359: Metallpulverspritzguss – Fertigung komplexer Bauteile in höchster Präzision, Verlag Moderne Industrie, Edition 1, 2013.

14. Majumdar J and Manna I. Laser material processing. International Materials Reviews 2011; 56 (5–6): 288–341.

15. Ho KH & Newman ST. State of the art electrical discharge machining (EDM). International Journal of Machine Tools & Manufacture 2003; 43: 1287–1300.

16. Flynn JM, Shokrani A, Newman ST and Dhokian V. Hybrid additive and subtractive machine tools – Research and industrial developments. International Journal of Machine Tools & Manufacture 2016; 101:79–101.

17. Hassanin H Modica F, El-Sayed M, Liu J and Essa K. Manufacturing of Ti–6Al–4V Micro-Implantable Parts Using Hybrid Selective Laser Melting and Micro-Electrical Discharge Machining. Advanced Engineering Materials 2016; 18(9): 1544-1549.

18. Hassanin H, Essa K, Qiu C, Abdelhafeez A, Adkins N and Attallah M. Net-shape manufacturing using hybrid selective laser melting/hot isostatic pressing. Rapid Prototyping Journal 2017; 23(4): 720-726.

19. Karunakaran KP, Suryakumar S, Pushpa V and Akula S. Low cost integration of additive and subtractive processes for hybrid layered manufacturing. Robotics and Computer-Integrated Manufacturing 2010; 26: 490-499.

20. Merklein M, Junker D, Schaub A and Neubauer F. Hybrid additive manufacturing technologies- An analysis regarding potentials and applications. Physics Procedia 2016; 83: 549-559.

21. Yamazaki T. Development of A Hybrid Multi-tasking Machine Tool: Integration of Additive Manufacturing Technology with CNC Machining. Procedia CIRP 2016; 42: 81 – 86.

22. Brøtan V and Bovie KM. The Hybrid Manufacturing Cell: Determining Key Parameters in the Integration of Powder Bed Fusion with High Speed Milling. In: The IEEE International Conference on Industrial Engineering and Engineering Management. ISBN 9781467329453; 2012, p. 583–587.

23. Penchev P, Bhaduri D, Dimov S, and Soo SL. Novel manufacturing platform for scale up production of miniaturized components. In: Proceedings of the 9th International Workshop on Microfactories, Honolulu, USA, 5-8 October 2014, pp.231-238.

24. Kerbrat O, Mognol P and Hascoet J-Y. A new DFM approach to combine machining and additive manufacturing. Computers in Industry 2011;62:684-692.

25. Um J, Rauch M, Hascoët JY and Stroud I. STEP-NC compliant process planning of additive manufacturing: remanufacturing. International Journal of Advanced Manufacturing Technologies 2017; 88:1215-1230.

26. Boivie K, Sørby K, Brøtan V and Ystgaard P. Development of a Hybrid Manufacturing Cell; Integration of Additive Manufacturing with CNC Machining," In: Twenty- Second Annual International Solid Freeform Fabrication Symposium - An Additive Manufacturing Conference, Austin, TX, USA, 2011, pp. 153-163.

27. Boivie K, Dolinšek S and Homar D. Hybrid Manufacturing: Integration of Additive Technologies for Competitive Production of Complex Tools and Products. In: Proceedings of the International Research/Expert Conference: Trends in the Development of Machinery and Associated Technology, Prague, Czech Republic, 2011, pp.53-56.

28. Penchev P, Dimov S, Bhaduri, D and Soo SL. Generic Integration Tools for Reconfigurable Laser Micromachining Systems. Journal of Manufacturing Systems 2016; 38:27–45.

29. Shang X, Penchev P, Guo C and et al. W-band waveguide filters fabricated by laser micromachining and 3-D printing. IEEE Trans Microw. Theory Techn. 2016; 64(8): 2572–2580.

30. Wu X. A review of laser fabrication of metallic engineering components and of materials. Materials Science and Technology 2007;23:631-640.

31. Sahasrabudhe H, Bose S and Bandyopadhyay A. Chapter 17 - Laser-Based Additive Manufacturing Processes. In: Advances in Laser Materials Processing (Second Edition). Woodhead Publishing, 2018, pp. 507-539.

32. Haruna WSW and et.al. A review of powder additive manufacturing processes for metallic biomaterials. Powder Technology 2018; 327:128-151.

33. Brøtana V, Fahlströmb J and Sørbya K. Industrialization of metal powder bed fusion through machine shop networking. Procedia CIRP 2016; 54: 181 – 185.

34. Zhu Z, Dhokia V and Newman ST. The development of a novel process planning algorithm for an unconstrained hybrid manufacturing process. Journal of Manufacturing Processes 2013;15(4): 404-413.

35. Newman ST, Zhu Z, Dhokia V and Shokrani A. Process planning for additive and subtractive manufacturing technologies. CIRP Annals 2015; 64(1): 467-470.

36. Ruan J, Eiamsa-ard K, Liou F. Automatic process planning and toolpath generation of a multiaxis hybrid manufacturing system. Journal of Manufacturing Processes 2005; 7:57–68.

37. Hu Z, Lee K. Concave edge-based part decomposition for hybrid rapid prototyping. International Journal of Machine Tools and Manufacture 2005;45:35–42.

38. Lee N and Joneja A. A methodology to improve manufacturing precision in the presence of workpiece imperfections. J Manuf Sci and Eng Trans ASEM 1997;119(4):616–622.

39. Systems 3R International AB. Instructions for Macro Control Ruler 3R- 606.1/-N. 2011, Vallingby, Sweden.

40. Penchev P, Dimov S, Bhaduri D, Soo SL and Crickboom B. Generic software tool for counteracting the dynamics effects of optical beam delivery systems. Proc IMechE Part B: J Engineering Manufacture 2017; 231(1): 48–64.

41. Bhaduri D, Penchev P, Dimov S and Soo SL. An investigation of accuracy, repeatability and reproducibility of laser micromachining systems. Measurement 2016; 88: 248-261.

42. ISO 1938-1:2015. Geometrical product specifications (GPS) -- Dimensional measuring equipment -- Part 1: Plain limit gauges of linear size.

43. Read N, Wang W, Essa K and Attallah MM. Selective laser melting of AlSi10Mg alloy: Process optimisation and mechanical properties development. Materials and Design 2015; 65: 417–424.

44. Alicona. Alicona Focus Variation magazine: From production measument technology to SmartManufacturing. Edition 8, 2018.

45. FARO. Faro Edge and ScanArm HD: Features, Benefits & Technical Specifications, http://www.b3-d.com/files/96731539.pdf

46. United Kingdom Accreditation Service (UKAS) M3003, The Expression of Uncertainty and Confidence in Measurement, Edition 2, 2007.